Supporting Information for

Magnetic-Field Controllable Displacement-Type Ferroelectricity Driven by Off-Center Fe^{2+} Ions in $CaFe_3Ti_4O_{12}$ Perovskite

Dabiao Lu,[1,2] Denis Sheptyakov,[3] Yingying Cao,[1,2] Haoting Zhao,[1,2] Jie Zhang,[1,2] Maocai Pi,[1,2] Xubin Ye,[1] Zhehong Liu,[1] Xueqiang Zhang,[1] Zhao Pan,[1] Xingxing Jiang,[4] Zhiwei Hu,[5] Yi-feng Yang,[1,2,6] Pu Yu,[7] and Youwen Long[1,2,6*]

[1]*Beijing National Laboratory for Condensed Matter Physics, Institute of Physics, Chinese Academy of Sciences, Beijing 100190, China*

[2]*School of Physical Sciences, University of Chinese Academy of Sciences, Beijing 100049, China*

[3]*Laboratory for Neutron Scattering and Imaging (LNS), Paul Scherrer Institut (PSI), Forschungsstrasse 111, CH-5232 Villigen, Switzerland*

[4]*Technical Institute of Physics and Chemistry, Chinese Academy of Sciences, Beijing 100190, China*

[5]*Max Planck Institute for Chemical Physics of Solids, Dresden 01187, Germany*

[6]*Songshan Lake Materials Laboratory, Dongguan, Guangdong 523808, China*

[7]*State Key Laboratory of Low Dimensional Quantum Physics and Department of Physics, Tsinghua University, Beijing, 100084, China*

*Corresponding email: ywlong@iphy.ac.cn

Table S1. Refined structure parameters of $CaFe_3Ti_4O_{12}$ based on the SXRD data collected at 290 K.

a (Å)	7.470873(2)
O_y	0.2984(1)
O_z	0.1887(1)
U_{iso} (Ca) (100×Å^2)	1.40(4)
U_{iso} (Fe) (100×Å^2)	2.54(2)
U_{iso} (Ti) (100×Å^2)	1.09(1)
U_{iso} (O) (100×Å^2)	0.94(1)
Ca-O (×12) (Å)	2.638(1)
Fe-O (×4) (Å)	2.0627(6)
	2.7707(6)
	3.2217(6)
Ti-O (×6) (Å)	1.9568(2)
Ti-O-Ti (°)	145.35(4)
Fe-O-Ti (°)	107.12(2)
BVS(Ca)	1.96
BVS(Fe)	1.96
BVS(Ti)	4.09
R_{wp} (%)	3.23
R_p (%)	2.19

The space group is *Im*-3 (No. 204), with atomic positions: Ca 2*a*(0, 0, 0), Fe 6*b*(0, 0.5, 0.5), Ti 8*c*(0.25, 0.25, 0.25), and O 24g(x, y, 0). The BVS values are calculated by using the formula $\sum_i \exp[(r_0 - r_i)/0.37]$, where r_i is the bond length, and r_0 is a constant for a specific ion. Here r_0 is 1.967 for Ca, 1.734 for Fe and 1.815 for Ti.

Table S2. Comparison of refined satisfactory goodness-of-fit parameters based on the SXRD pattern collected at 5 K using different space groups for $CaFe_3Ti_4O_{12}$

Space group	χ^2	R_{wp} (%)	R_p (%)
Im-3	0.1256	4.54	2.87
*R*3	0.0670	4.09	2.46
*Imm*2	0.0779	4.06	2.56

Table S3. Refined structure parameters of $CaFe_3Ti_4O_{12}$ based on the SXRD data collected at 5 K.

Atom	site	x	y	z	Uiso (100×Å^2)
Ca	3*a*	0	0	-0.0050(8)	0.87(2)
Fe	9*b*	0.1556(3)	0.3378(3)	0.3312(4)	3.62(1)
Ti1	3*a*	0	0	0.4951(7)	0.30(1)
Ti2	9*b*	0.5008(2)	-0.0024(4)	0.4894(4)	2.13(1)
O1	9*b*	0.2271(7)	0.2641(5)	0.0892(8)	0.93(5)
O2	9*b*	0.1551(4)	0.1693(6)	0.6904(7)	1.22(7)
O3	9*b*	0.1693(5)	0.0308(4)	0.3424(9)	0.11(4)
O4	9*b*	0.1208(4)	0.4189(6)	0.6421(7)	4.72(9)

Space group: $R3$ (No. 146), a = 10.55453(3) Å, c = 6.46314(4) Å, R_{wp} = 4.09%, R_{p} = 2.46%.

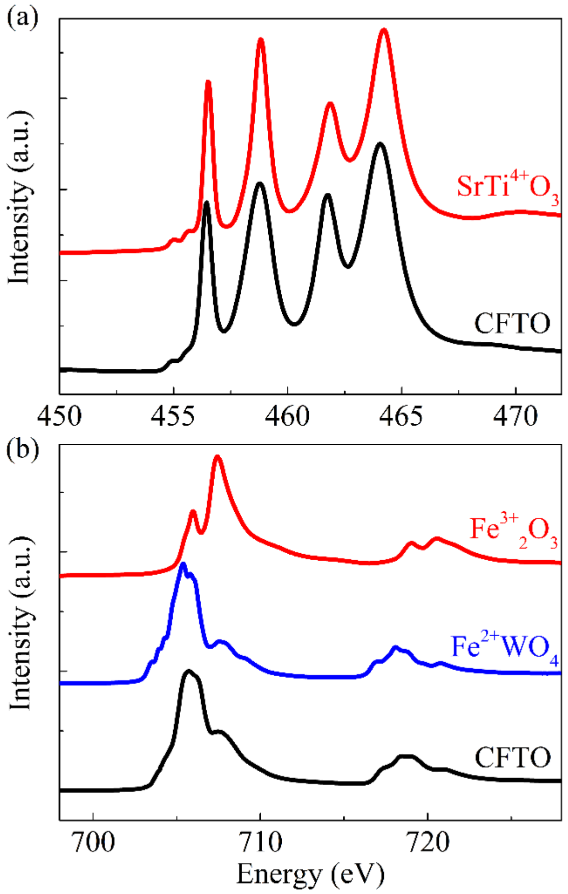

Figure S1. X-ray absorption spectroscopy for $CaFe_3Ti_4O_{12}$ (CFTO) measured at room temperature. (a) Ti-$L_{2,3}$ edges of CFTO and reference $SrTiO_3$. Their similar spectral shapes and energy positions confirm the Ti^{4+} charge state in CFTO. (b) Fe-$L_{2,3}$ edges of CFTO and two references Fe_2O_3 and $FeWO_4$[1] with Fe^{3+} and Fe^{2+} charge states, respectively. The similar energy positions and peak profiles between CFTO and $FeWO_4$ confirm the Fe^{2+} charge state in CFTO.

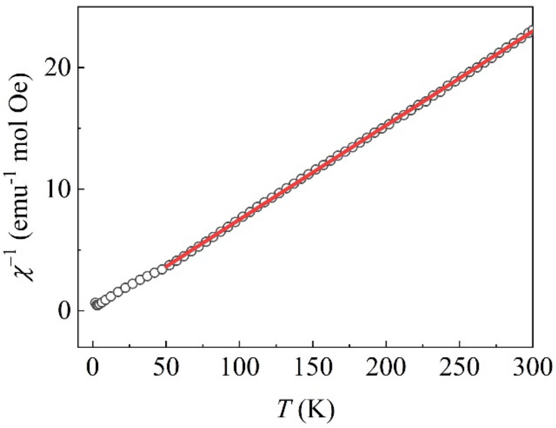

Figure S2. The Curie–Weiss fitting for the zero-field cooling (ZFC) data of χ^{-1} above 50 K using the function $\chi^{-1} = (T - \theta) / C$ for $CaFe_3Ti_4O_{12}$. The absolute value of the fitted Weiss temperature θ (= -3.19 K) is comparable to $T_N \approx 3.1$ K, and the negative sign agrees with the antiferromagnetic interaction. According to the fitted Curie Constant C (= 12.91 emu K Oe^{-1} mol^{-1}), the effective magnetic moment is calculated as 10.13 μ_B f.u.$^{-1}$. This value is somewhat larger than the theoretical one (8.57 μ_B f.u.$^{-1}$), if we only consider the contribution of the spin moment for a high-spin Fe^{2+}. The possible reasons are the presence of some magnetic moments at the oxygen sites owing to the presence of strong Fe–O covalent effects [2] and existence of the orbital contribution as proposed to explain the higher-than-expected effective Co^{2+} moment in isostructural $CaCo_3Ti_4O_{12}$ [3].

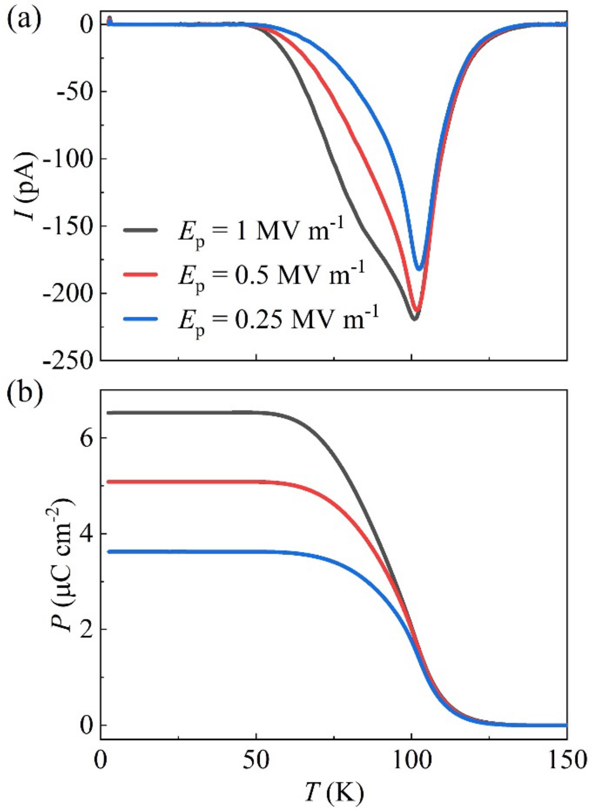

Figure S3. Temperature dependent (a) pyroelectric current and (b) corresponding polarization measured under different poling fields E_p. The pyroelectric current and the polarization increase with increasing poling fields, implying the polarization is not saturated, consistent with the PE loop results.

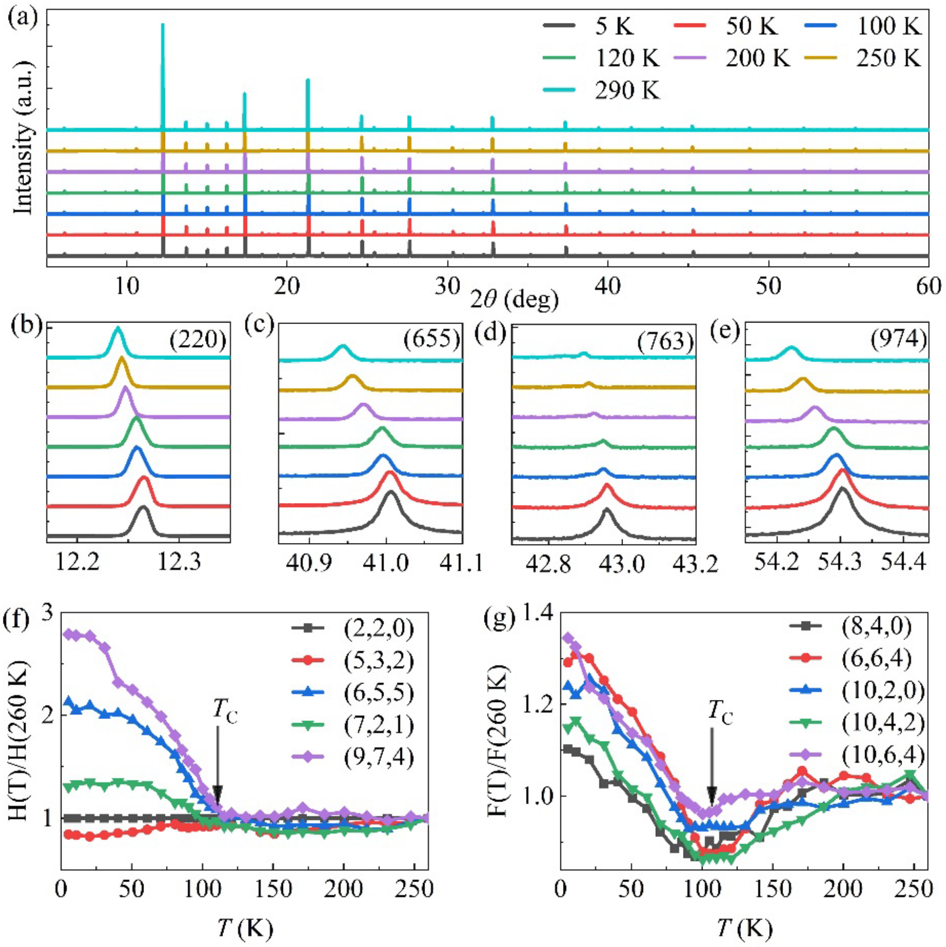

Figure S4. (a) SXRD patterns measured at some representative temperatures for $CaFe_3Ti_4O_{12}$. (b-e) Enlarge view of SXRD patterns for some characteristic diffraction peaks. Temperature dependence of, (f) peak height H(T), (g) full width at half maximum (FWHM) F(T) of some characteristic diffraction peaks.

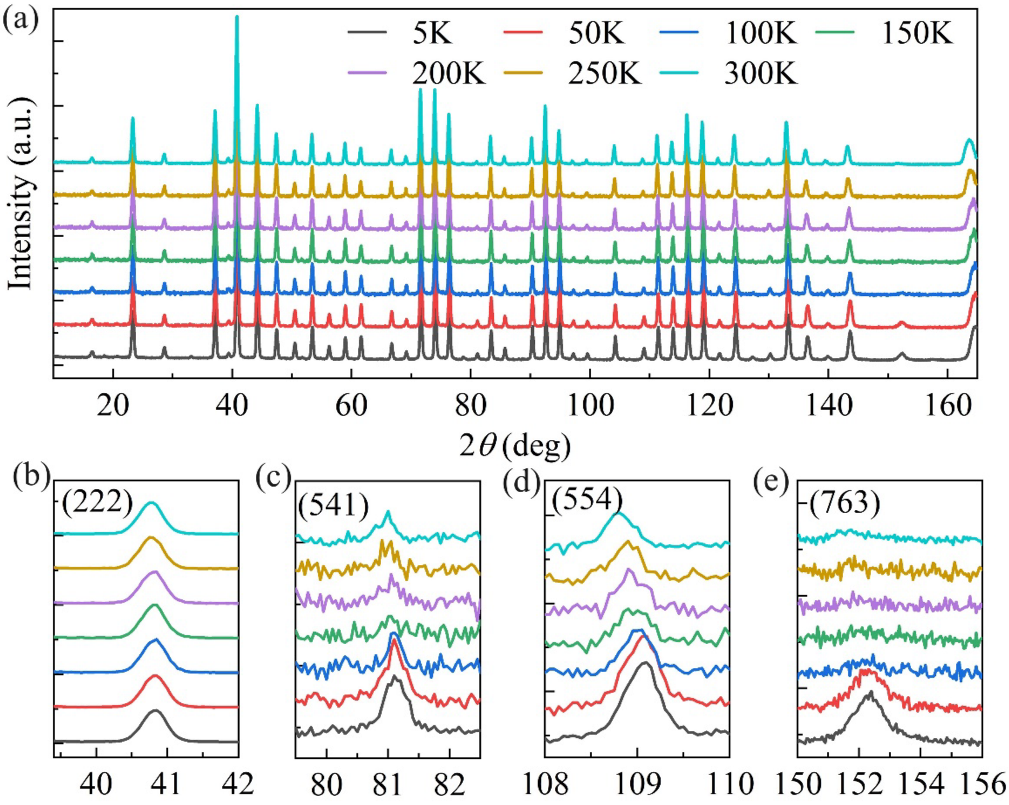

Figure S5. (a) NPD patterns measured at some representative temperatures with a wavelength of 1.494 Å for $CaFe_3Ti_4O_{12}$. (b-e) Enlarge view of NPD patterns for some characteristic diffraction peaks. The relative intensities of some diffraction peaks increase remarkably below T_C, implying a structural transition.

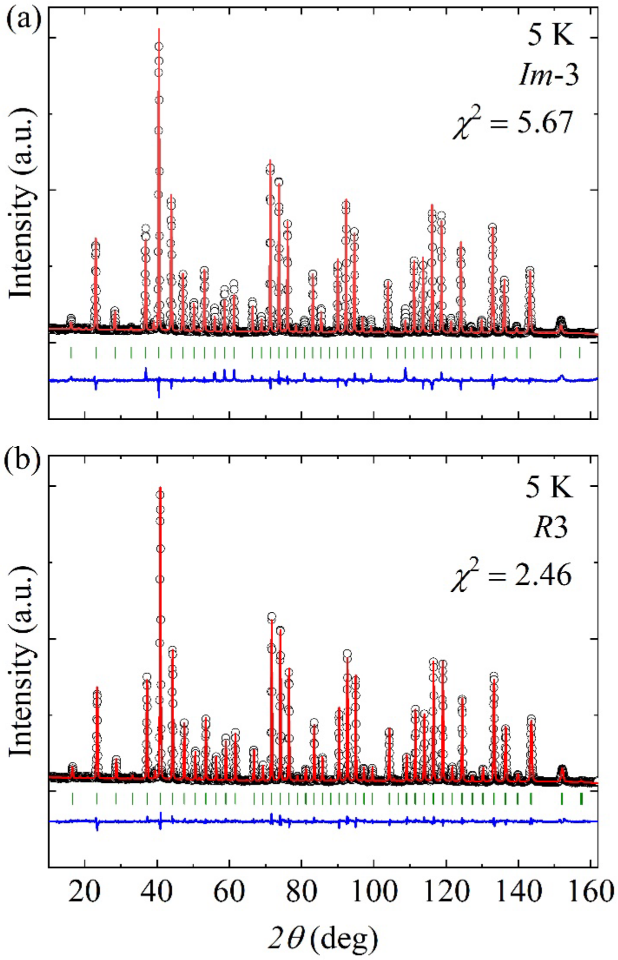

Figure S6. Rietveld refinement results based on the NPD data collected at 5 K using the (a) *Im*-3 and (b) *R*3 space group. Observed (black circles), calculated (red line), and difference (blue line) are illustrated. The green ticks indicate the allowed Bragg reflections. Compared with the refinement quality by using *Im*-3 space group, significant improvement can be achieved by using *R*3 space group.

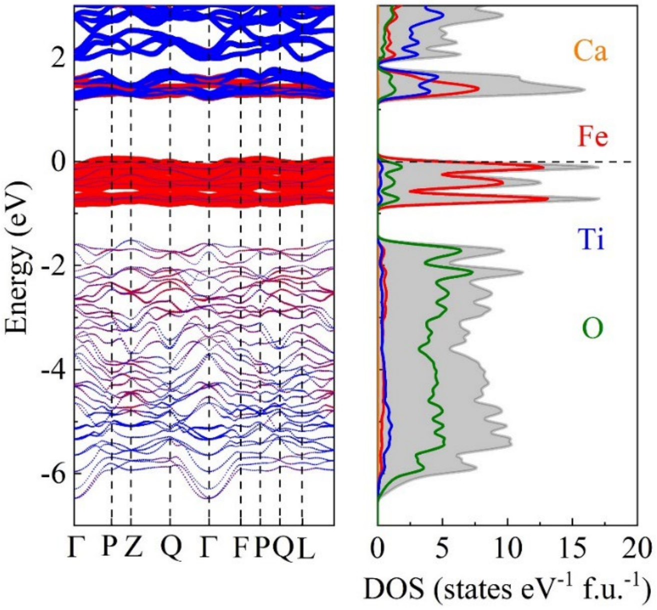

Figure S7. First-principles calculation results for the band structures and density of states (DOS) for $CaFe_3Ti_4O_{12}$ with the polarized *R*3 symmetry. The total DOS (light gray) and partial DOS of Ca (orange curves), Fe (red curves), Ti (blue curves), and O (green curves) are all shown for comparison.

Reference

1. Maignan A., Schmidt M., Prots Y. *et al.* $FeWO_4$ Single Crystals: Structure, Oxidation States, and Magnetic and Transport Properties. *Chem. Mater.* 2022; 34; 789- 97.
2. Li H., Lv S., Han L. *et al.* First-principles investigation of magnetic coupling mechanism in A-site-ordered perovskite $CaFe_3Ti_4O_{12}$. *Comp. Mater. Sci*. 2012; **53**: 329-32.
3. Amano P. M., Denis R. F., Koo H.-J. *et al*. Orthogonal antiferromagnetism to canted ferromagnetism in $CaCo_3Ti_4O_{12}$ quadruple perovskite driven by underlying kagome lattices. *Commun. Mater*. 2022; **3**: 51.